

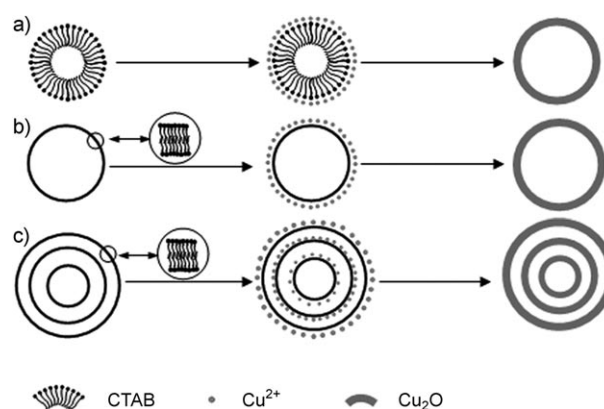
# Template Synthesis of Multishelled $\text{Cu}_2\text{O}$ Hollow Spheres with a Single-Crystalline Shell Wall\*\*

Haolan Xu and Wenzhong Wang\*

Nanomaterials are attracting increasing attention due to their potential applications and enhanced properties. It is well known, for instance, that the size, morphology, and structure of nanomaterials significantly influence their physical and chemical properties and, therefore, their applications.<sup>[1]</sup> Extensive studies have been devoted to the controlled synthesis of nanocrystals in the past few decades, and hollow nanostructures are of particular interest owing to potential applications such as drug delivery, artificial cells, lightweight fillers, catalysis, and chemical storage.<sup>[2,3]</sup> Various methodologies have been developed to achieve this special nanostructure. Template synthesis, for example, is a typical and effective route, and hard or soft templates, such as polymeric core supports, silica spheres, vesicles, and liquid droplets, have been applied.<sup>[2-4]</sup> However, the resulting hollow spheres are generally single-shelled and polycrystalline. Recently, polycrystalline double-shelled hollow spheres have been synthesized by using hollow latex and polymer spheres as templates.<sup>[5]</sup> The synthesis of hollow structured materials with a single-crystalline shell wall, designable inner space, and a complex structure (such as multishelled) will further extend their applications, although it remains a technological challenge.<sup>[6]</sup>

The self-assembly of surfactant molecules in aqueous solution leads to the formation of micelles and closed bilayer aggregates such as vesicles (also referred to as organized molecular assemblies) or dynamic nanostructures of surfactant molecules. Much effort has been devoted to the study and preparation of vesicles because they can be widely applied as delivery vehicles in the pharmaceutical and cosmetic industries and also as soft templates for the transcriptive synthesis of organic and inorganic hollow spheres.<sup>[7]</sup> Since the bilayer structures separate an aqueous interior from an aqueous

exterior, the interface between the surfactant groups and the solution presents a specific site for the growth of materials from solution. Crystal growth and solidification at the interface leads to transcriptive imprinting of the template morphology and the formation of hollow structured materials. Some vesicles such as dioctadecyldimethylammonium bromide (DODAB),<sup>[8]</sup> poly(diallyldimethylammonium) chloride (PDADMAC),<sup>[2b]</sup> and mixtures of dodecyltrimethylammonium bromide (DTAB) and sodium dodecylbenzenesulfonate (SDBS),<sup>[9]</sup> have been successfully used to synthesize inorganic single-shelled hollow spheres. Scheme 1a,b illustrates the



**Scheme 1.** The formation of different  $\text{Cu}_2\text{O}$  hollow structures in the presence of a CTAB template: a) micelle, b) single-lamellar vesicle, c) multilamellar vesicle.

formation of single-shelled inorganic hollow spheres by using micelles and vesicles as templates. Theoretically, it is possible for all the layers of the multilamellar vesicle to serve as growth sites (as shown in Scheme 1c), which should lead to multishelled hollow spheres. However, this hollow structure transcriptive imprinting from multilamellar vesicles has never been realized before. Herein, we report the first successful synthesis of double- and even triple- and quadruple-shelled hollow spheres by using cetyltrimethylammonium bromide (CTAB) multilamellar vesicles as soft templates. The shells of these hollow spheres are single-crystalline; this property has rarely been reported before and makes these structures more stable. Scheme 1c illustrates the possible processes for the formation of the triple- and quadruple-shelled hollow spheres.

The use of vesicles as templates for the transcriptive synthesis of hollow nanostructures is not trivial.<sup>[8]</sup> Since the structures of the vesicle templates are sensitive to many parameters, such as pH, temperature, concentration, solvent, inorganic additives, and ionic strength, we decided to control the structure of these hollow spheres (the number of shells)

[\*] H. Xu, Prof. W. Wang

State Key Laboratory of High Performance Ceramics and Superfine Microstructure Shanghai Institute of Ceramics  
Chinese Academy of Science  
1295 Dingxi Road Shanghai 200050 (P. R. China)

and

Graduate School of Chinese Academy of Sciences  
Shanghai 200050 (P. R. China)

Fax: (+86) 215-241-3122

E-mail: wzwang@mail.sic.ac.cn

[\*\*] Financial support from the Chinese Academy of Sciences and the Shanghai Institute of Ceramics under the program for Recruiting Outstanding Overseas Chinese (Hundred Talents Program) is gratefully acknowledged. We also thank the National Natural Science Foundation of China (no. 50672117).

Supporting Information for this article is available on the WWW under <http://www.angewandte.org> or from the author.

simply by adjusting the concentration of CTAB whilst keeping the other conditions constant. TEM images were recorded to investigate the evolution of the morphologies and structures of the products that accompany the change of surfactant concentration. When the concentration of CTAB reaches 0.08 M, the hollow nanostructured product  $\text{Cu}_2\text{O}$  appears (see Figure S1 in the Supporting Information), which implies that CTAB micelles or vesicles are produced at this concentration. When the concentration of CTAB is increased to 0.1 M, the morphology of the as-prepared  $\text{Cu}_2\text{O}$  is that of uniform single-shelled hollow spheres with a diameter of about 100–120 nm (Figure 1 a). The thickness of the shell is estimated to be about 20–25 nm. The clear two-dimensional lattice fringes

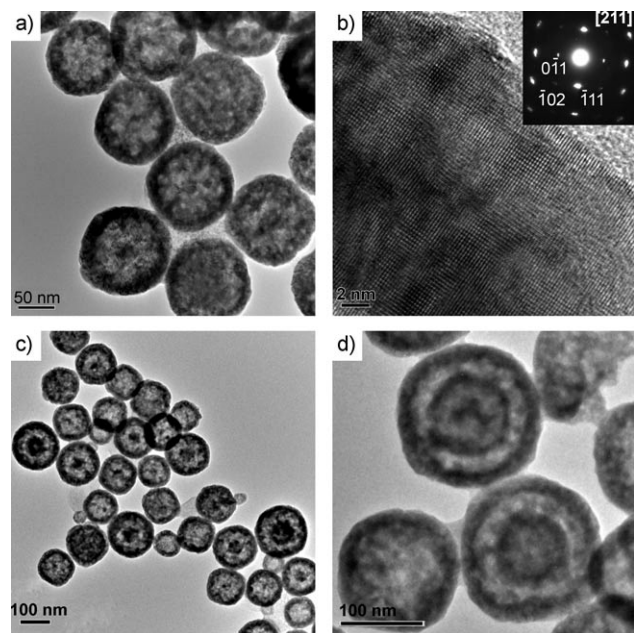


**Figure 1.** TEM and HRTEM images of the  $\text{Cu}_2\text{O}$  hollow spheres prepared at a CTAB concentration of 0.1 M: a) TEM image of single-shelled  $\text{Cu}_2\text{O}$  hollow spheres, b) HRTEM image of the shell wall (inset: corresponding SAED pattern), c) TEM image of the product in a panoramic view, d) TEM image of two double-shelled  $\text{Cu}_2\text{O}$  hollow spheres.

that are apparent in the high-resolution (HR) TEM image (Figure 1 b) confirm the single-crystallinity of the shell. The selected-area electron diffraction (SAED) pattern of a single-shelled  $\text{Cu}_2\text{O}$  hollow sphere (inset in Figure 1 b) can be indexed to the [211] zone axis of cubic  $\text{Cu}_2\text{O}$ , which further confirms that the shell walls of the hollow spheres are single-crystalline. The single-crystalline nature of the hollow spheres shells should improve their stability and may give rise to specific applications in further studies. These single-shelled  $\text{Cu}_2\text{O}$  hollow spheres may form with the assistance of CTAB micelles, an assembled monolayer structure of CTAB surfactant molecules. As illustrated in Scheme 1 a, CTAB micelles are produced initially when the solution is heated. Cu–Br moieties then form by electrostatic interaction of  $\text{Cu}^{2+}$  and  $\text{Br}^-$  (from CTAB), which leads to an enrichment of  $\text{Cu}^{2+}$  at the interface between the hydrophilic groups of CTAB and

the aqueous solution.  $\text{Cu}^{2+}$  is then reduced to  $\text{Cu}_2\text{O}$  and Ostwald ripening occurs. Thus, the shape of the micelle is replicated. In addition, unilamellar CTAB vesicles may also direct the formation of single-shelled  $\text{Cu}_2\text{O}$  hollow spheres. This process is summarized in Scheme 1 b and has been widely reported in the literature.<sup>[2b,7a,8,9]</sup>

A view of the product (Figure 1 c) shows the coexistence of double- and single-shelled hollow  $\text{Cu}_2\text{O}$  spheres, although the latter is the dominant structure. Figure 1 d shows a TEM image of a double-shelled  $\text{Cu}_2\text{O}$  hollow sphere at high magnification. The obvious contrast between the dark edges and the pale center confirms the double-shelled hollow structure. The size of the double-shelled  $\text{Cu}_2\text{O}$  hollow spheres was estimated to be about 150–180 nm, which is larger than that of the single-shelled hollow spheres. The size of the inner hollow spheres is about 80–90 nm, which is a little smaller than that of a single-shelled hollow sphere.

Similar to the formation of single-shelled  $\text{Cu}_2\text{O}$  hollow spheres (Scheme 1 a,b), double-shelled  $\text{Cu}_2\text{O}$  hollow spheres are formed with the assistance of double-lamellar CTAB vesicles, which have two layers of assembled bilayers. In this particular structure,  $\text{Cu}_2\text{O}$  can grow on both layers, which leads to the formation of a double-shelled  $\text{Cu}_2\text{O}$  hollow sphere. The space between the layers of the double-lamellar vesicle corresponds to the shell space of the double-shelled  $\text{Cu}_2\text{O}$  hollow sphere; therefore, the coexistence of single- and double-shelled  $\text{Cu}_2\text{O}$  hollow spheres (Figure 1 c) implies the presence of some double-lamellar CTAB vesicles along with the dominant CTAB micelles or unilamellar vesicles. A dynamic light scattering (DLS) study of the CTAB solution (0.1 M in the presence of Cu ions and ascorbic acid at 60 °C) confirmed the existence of CTAB assembled structures (see Figure S2 in the Supporting Information). The corresponding size distribution indicates the structural difference between the micelles and vesicles. It is well known that an increase of surfactant concentration will drive the conversion from micelles to vesicles and multilamellar vesicles. Thus, when the concentration of CTAB is increased we should obtain more multilamellar CTAB vesicles and the amount of double-shelled  $\text{Cu}_2\text{O}$  hollow spheres should also increase. To confirm this, another experiment was carried out where the concentration of CTAB was increased to 0.13 M (the other experimental conditions were kept constant). The view of the product shown in Figure 2 a shows that the dominant structure is now that of double-shelled hollow spheres. The double-shelled structure was further confirmed by the SEM image (Figure 2 b), which shows a cracked  $\text{Cu}_2\text{O}$  hollow sphere where the inner sphere can clearly be seen through the broken shell. The walls of these double-shelled hollow spheres are also single-crystalline, as shown by the HRTEM image and SAED pattern (inset) in Figure 2 c. Interestingly, triple-shelled  $\text{Cu}_2\text{O}$  hollow spheres are also observed, although they are very few in number. Figure 2 d shows the TEM image of a triple-shelled  $\text{Cu}_2\text{O}$  hollow sphere at high magnification; its unique structure is clearly revealed. The diameters of the single-, double-, and triple-shelled  $\text{Cu}_2\text{O}$  hollow spheres are about 100–120, 150–180, and 210–240 nm, respectively. This indicates that hollow spheres with the same structure have similar sizes.

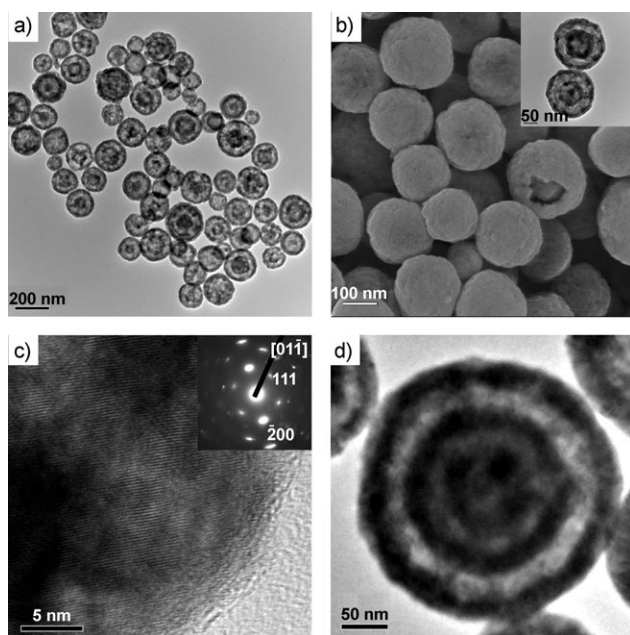


**Figure 2.** TEM and SEM images of the  $\text{Cu}_2\text{O}$  hollow spheres prepared at a CTAB concentration of 0.13 M: a) TEM image of double-shelled  $\text{Cu}_2\text{O}$  hollow spheres, b) SEM image of the product (inset: corresponding TEM image), c) HRTEM image of the shell wall (inset: corresponding SAED pattern), d) TEM image of a triple-shelled  $\text{Cu}_2\text{O}$  hollow sphere.

The formation of triple-shelled  $\text{Cu}_2\text{O}$  hollow spheres implies the existence of triple-lamellar CTAB vesicles (Scheme 1c). These have a higher ordered molecular structure that evolves from double-lamellar vesicles upon increasing the concentration of CTAB. When the concentration of CTAB was further raised to 0.15 M, the number of triple-shelled hollow  $\text{Cu}_2\text{O}$  spheres also increased. Figure 3a shows a typical TEM image of the triple-shelled  $\text{Cu}_2\text{O}$  hollow spheres. The corresponding SEM image (Figure 3b) shows a cracked triple-shelled sphere. Two of the outer shells of this hollow sphere are cracked, which permits us to observe the inner sphere directly. In accordance with the analysis of the previous TEM images, we can conclude that  $\text{Cu}_2\text{O}$  hollow spheres with the same structure (number of shells) are of similar size. By using the size of the cracked triple-shelled  $\text{Cu}_2\text{O}$  hollow sphere (230–260 nm) as a criterion, we can estimate that about 40% of the  $\text{Cu}_2\text{O}$  particles are triple-shelled hollow spheres (Figure 3c) and a further 40% are double-shelled hollow spheres. There are also about 5%  $\text{Cu}_2\text{O}$  spheres with a diameter of approximately 300 nm. These should be more complex quadruple-shelled hollow spheres, as confirmed by the TEM images shown in Figure 3d, from which a diameter of about 290 nm was determined.

In summary, we have developed a facile method to synthesize novel hollow nanostructures (multishelled hollow spheres) with the assistance of CTAB vesicles and multilamellar vesicles. The structure (single-, double-, triple-, and quadruple-shelled) of these  $\text{Cu}_2\text{O}$  hollow spheres can be easily controlled by adjusting the concentration of the CTAB surfactant. The HRTEM images have revealed that the shells of these hollow spheres are single-crystalline, which may improve their stability. Our report confirms the feasibility of

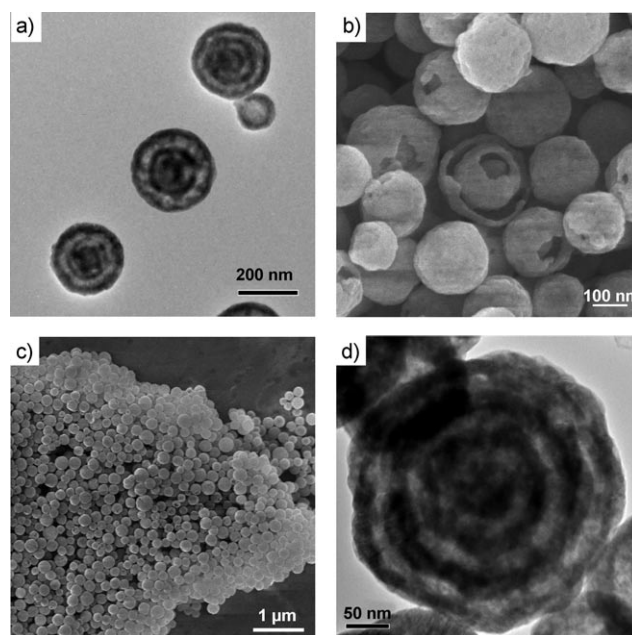


**Figure 3.** TEM and SEM images of the  $\text{Cu}_2\text{O}$  hollow spheres prepared at a CTAB concentration of 0.15 M: a) TEM image of the triple-shelled  $\text{Cu}_2\text{O}$  hollow spheres, b) SEM image of the triple-shelled  $\text{Cu}_2\text{O}$  hollow spheres, c) SEM image of the product at low magnification, d) TEM image of a quadruple-shelled hollow sphere.

vesicle and multilamellar vesicle directed synthesis of inorganic multishelled hollow spheres. Considering that the formation of these multishelled hollow structures as well as their single-crystalline shell wall may involve more than one process, the detailed mechanism needs to be studied in more depth. These hierarchical hollow spheres may have uses in the fields of carriers and drug release with prolonged release time. More importantly, it may prove possible to create multifunctional materials by filling different target materials into different chambers of the multishelled hollow spheres.

### Experimental Section

In a typical procedure,  $\text{CuSO}_4 \cdot 5\text{H}_2\text{O}$  (0.05 g) was dissolved in 100 mL of CTAB solution with different concentrations (0.1, 0.13, and 0.15 M in water). Ascorbic acid (0.18 g) was then added and the solution was heated to 60°C and kept at that temperature for 20 min. A yellow precipitate of  $\text{Cu}_2\text{O}$  was produced when 10 mL of NaOH solution (0.2 M in water) was added dropwise to the above solution. After stirring for 10 min the precipitate was centrifuged, washed sequentially with deionized water and ethanol several times, and then dried at 50°C for 5 h under vacuum. The XRD pattern of the  $\text{Cu}_2\text{O}$  product is given as Supporting Information.

The XRD pattern was recorded with a D/MAX 2250 V diffractometer (Rigaku, Japan) using  $\text{Cu}_{\text{K}\alpha}$  radiation ( $\lambda = 1.5406 \text{ \AA}$ ). The morphologies and microstructures of the products were investigated by TEM (JEM-2100F) and field emission SEM (JSM-6700F). The size distribution of the CTAB vesicles was analyzed by DLS with a zeta-potential analyzer (Zeta Plus, Brookhaven Instruments Corporation).

Received: September 22, 2006

Revised: November 14, 2006

Published online: January 17, 2007

**Keywords:** copper · materials science · nanostructures · template synthesis · vesicles

- 
- [1] a) A. P. Alivisatos, *Science* **1996**, *271*, 933; b) M. A. El-Sayed, *Acc. Chem. Res.* **2001**, *34*, 257; c) J. T. Hu, T. W. Odom, C. M. Lieber, *Acc. Chem. Res.* **1999**, *32*, 435.
- [2] a) F. Caruso, R. A. Caruso, H. Möhwald, *Science* **1998**, *282*, 1111; b) F. Caruso, *Chem. Eur. J.* **2000**, *6*, 413; c) F. Caruso, *Adv. Mater.* **2001**, *13*, 11.
- [3] a) C. G. Göltner, *Angew. Chem.* **1999**, *111*, 3347; *Angew. Chem. Int. Ed.* **1999**, *38*, 3155; b) Z. Y. Zhong, Y. D. Yin, B. Gates, Y. N. Xia, *Adv. Mater.* **2000**, *12*, 206; c) Y. G. Sun, Y. N. Xia, *Science* **2002**, *298*, 2176.
- [4] a) A. D. Dinsmore, M. F. Hsu, M. G. Nikolaidis, M. Marquez, A. R. Bausch, D. A. Weitz, *Science* **2002**, *298*, 1006; b) T. Nakashima, N. Kimizuka, *J. Am. Chem. Soc.* **2003**, *125*, 6386; c) H. G. Yang, H. C. Zeng, *Angew. Chem.* **2004**, *116*, 5318; *Angew. Chem. Int. Ed.* **2004**, *43*, 5206; d) Z. Z. Yang, Z. W. Niu, Y. F. Lu, Z. B. Hu, C. C. Han, *Angew. Chem.* **2003**, *115*, 1987; *Angew. Chem. Int. Ed.* **2003**, *42*, 1943.
- [5] a) M. Yang, J. Ma, Z. W. Niu, X. Dong, H. F. Xu, Z. K. Meng, Z. G. Jin, Y. F. Lu, Z. B. Hu, Z. Z. Yang, *Adv. Funct. Mater.* **2005**, *15*, 1523; b) M. Yang, J. Ma, C. L. Zhang, Z. Z. Yang, Y. F. Lu, *Angew. Chem.* **2005**, *117*, 6885; *Angew. Chem. Int. Ed.* **2005**, *44*, 6727.
- [6] a) H. L. Xu, W. Z. Wang, W. Zhu, L. Zhou, *Nanotechnology* **2006**, *17*, 3649; b) H. G. Yang, H. C. Zeng, *Angew. Chem.* **2004**, *116*, 6056; *Angew. Chem. Int. Ed.* **2004**, *43*, 5930.
- [7] a) D. H. W. Hubert, M. Jung, A. L. German, *Adv. Mater.* **2000**, *12*, 1291; b) J. Hotz, W. Meier, *Langmuir* **1998**, *14*, 1031.
- [8] D. H. W. Hubert, M. Jung, P. M. Frederik, P. H. H. Bomans, J. Meuldijk, A. L. German, *Adv. Mater.* **2000**, *12*, 1286.
- [9] M. Kepczynski, F. Ganachaud, P. Hemery, *Adv. Mater.* **2004**, *16*, 1861.
-